Ceramics International 44 (2018) 5939–5944

Contents lists available at ScienceDirect

Ceramics International

journal homepage: www.elsevier.com/locate/ceramint

α- and β-$AgVO_3$ polymorphs as photoluminescent materials: An example of temperature-driven synthesis

Regiane Cristina Oliveira[a], Mayara Mondego Teixeira[a], João Paulo C. Costa[a], Maya Penha[a], Eric Mark Francisco[a], Jussara Soares da Silva[a], Máximo Siu Li[b], Elson Longo[a,*], Lourdes Gracia[c], Juan Andrés[d]

[a] INCTMN-CDMF, Universidade Federal de São Carlos, P.O. Box 676, 13565-905 São Carlos, SP, Brazil
[b] IFSC-Universidade de São Paulo, P.O. Box 369, 13560-970 São Carlos, São Paulo, Brazil
[c] Departament de Química Física i Analítica, University of Valencia, 46100 Burjassot, Spain
[d] Departament de Química Física i Analítica, University Jaume I, 12071 Castellón, Spain

ARTICLE INFO

Keywords:
Polymorphism
α-$AgVO_3$
β-$AgVO_3$
Photoluminescence

ABSTRACT

Controlling the synthesis of a given polymorph of an inorganic material is a further step in the design of property and function. In this letter, we report for the first time a simple procedure to effectively control the reversible transformation between the crystalline polymorphs α-$AgVO_3$ and β-$AgVO_3$. Photoluminescence emission (PL) performance is analyzed; at low temperatures (up to 35 °C) when α-$AgVO_3$ is formed the PL emission is red, while at temperatures larger than 45 °C when β-$AgVO_3$ is obtained the color of emission PL emission goes from green to blue. The findings highlight the ability of temperature to dramatically alter the nature of phase transformation at the atomic level. The phase transformation is driven by the short-range structural and electronic changes of [VO_4] and [AgO_x] (x = 5, 6, and 7) clusters (building blocks of both monoclinic structures), and hence is dependent on the temperature employed during synthesis. These outcomes clearly demonstrate that the $AgVO_3$ crystals exhibited appropriate activity for application in visible lamps, displays, and other optical devices.

1. Introduction

The development of new applications has driven the field of materials design and synthesis to investigate materials that are not thermodynamically stable, i.e., metastable phases of one compound with different crystal structures [1]. These metastable phases are increasingly important because each polymorph can present unexplored physical and chemical properties that are distinct from the properties of their thermodynamically stable counterparts and will be vital in applications [2].

In solid-state chemistry, a major challenge appears in establishing controllable synthesis routes towards metastable polymorphs because there are limited numbers of very deep minima on the potential energy surface corresponding to a given stoichiometry in the phase diagram. Solid-state synthesis methods typically rely on equilibrium routes; non-equilibrium or metastable phases may be attained by quenching an intermediate of the reaction or by particular synthesis procedures such as gas phase, hydrothermal, mechanochemical, or template synthesis [3]. However, these procedures suffer from difficulties in rational handling for function design. Thus, the formation of such metastable materials requires complete understanding of their chemical and physical properties through state of the art experimental or theoretical investigation. In this respect, unravelling the relationship between the atomic structure and the functional properties can be a crucial step, especially in complex materials where short-range interactions rather than the average structure can define their actual properties and behaviors.

$AgVO_3$ is the most commonly occurring silver vanadium oxide-based material in the solid state [4] and has attracted interest owing to its technological applications in areas such as lithium ion batteries, antibacterial agents, sensors, and optical materials [5–14]. $AgVO_3$ has two phases that correspond to the metastable α-$AgVO_3$ and stable β-$AgVO_3$ phases with monoclinic space groups *Cm* and *C2/c*, respectively. α-$AgVO_3$ can be irreversibly transformed to β-$AgVO_3$ at around 200 °C [13,15]. To date, the procedure regarded as optimal for the preparation of the stable β-phase of $AgVO_3$ is a co-precipitation process at ambient temperature [13,16]. Syntheses of metastable α-$AgVO_3$ have either reported poorly crystalline samples and demanding requirements such

* Corresponding author.
E-mail address: elson.liec@gmail.com (R.C. Oliveira).

https://doi.org/10.1016/j.ceramint.2017.12.161
Received 26 October 2017; Received in revised form 19 December 2017; Accepted 22 December 2017
Available online 02 January 2018

as high temperatures or long reaction times [13,17,18], while Shao *et al*. successfully synthesized pure α-$AgVO_3$ with high crystallinity through a biomimetic process [19]. Very recently, α-$AgVO_3$ nanowires decorated with Ag nanoparticles were successfully prepared by hydrothermal treatment of a mixture of ammonium metavanadate and silver nitrate. Heating the as-prepared nanowires to 475 °C in N_2 results in a structural conversion from α-$AgVO_3$ to β-$AgVO_3$ for application as cathode material in Li-ion batteries [20]. It has previously been suggested that the electrochemical performance of β-$AgVO_3$ is superior to that of α-$AgVO_3$ due to a unique tunnel structure that accommodates cations [5,12].

Interest from a basic scientific viewpoint is fueled by novel synthesis routes to a stable phase, β-$AgVO_3$ [16] and a metastable phase, α-$AgVO_3$ [21]. In particular, we have achieved the synthesis of α-$AgVO_3$ powders using a co-precipitation method at 10, 20, and 30 °C [16,21]. These polymorphs possess coordination environments for Ag and V cations that are highly sensitive to variations in temperature, pressure, irradiation, doping, and particle size. This characteristic allows evaluation of the structural and electronic disorder behaviors and correlations with bonding and structural characters. Encouraged by the findings from these recent experimental/theoretical works, in this work, we first report the temperature-controllable phase transformation of $AgVO_3$ in solid-state material that is manipulated so that the system evolves via the lowest barrier path. Though frequent in molecular chemistry, this process is uncommon in solid-state chemistry.

Herein, we prepare $AgVO_3$ by co-precipitation and polymorphic control of this complex metal oxide is reached by tuning the reaction temperature. As a result, structural transformation between the two different monoclinic and crystalline phases (α-unstable and β-stable) of $AgVO_3$ was realized. In addition, photoluminescence (PL) emission offers a wide range of colors from red to blue as a function of temperature, suggesting $AgVO_3$ crystals are a promising candidate for optical material in technological applications. The PL behavior can be correlated to the structural and electronic changes at short range of the [VO_4] and [AgO_x] (x = 5, 6, and 7) clusters, which are building blocks of the monoclinic structures of both phases.

2. Method

2.1. Synthesis of $AgVO_3$ crystals

The $AgVO_3$ crystals were obtained by controlled co-precipitation method at 0, 15, 25, 35, 45, 65, ad 75 °C for 10 min. The precursors utilized in this synthesis were silver nitrate, $AgNO_3$ (99% purity, Synth) and ammonium monovanadate, NH_4VO_3 (99% purity, Aldrich). 1 mmol de NH_4VO_3 was dissolved in 60 mL distilled water at 30 °C, under magnetic stirring for 15 min, and 1 mmol of $AgNO_3$ was dissolved in 15 mL distilled water, under magnetic stirring for 15 min. Both solutions were placed in an ice bath at 0 °C and quickly mixed promoting the instantaneous formation $AgVO_3$ precipitate (for the synthesis at 0 °C). The other synthesis was carried out by varying the temperature using a heating plate. A magnetic stirrer with heating (IKA HS 7) coupled to a thermocouple (ETS-D6), which according to the manufacturer has accuracy of temperature measurement: ± 0.05 + tolerance PT1000 (DIN IEC 751 Class A). The precipitated was washed with distilled water several times, and drying in a conventional furnace at 60 °C for 10 h.

2.2. Characterization

The $AgVO_3$ crystals were characterized by XRD using $Cu_{K\alpha}$ radiation (λ = 1.5406 Å) (Rigaku diffractometer, Model D/Max-2500PC, Japan) in the 2θ range of 10–80° at a scan speed of rate of 2°/min. The morphology was investigated with a field emission scanning electron microscope (FE-SEM) Supra 35-VP Carl Zeiss (Germany) operating at 15 kV. The PL measurements were performed with a Monospec 27 monochromator (Thermal Jarrel Ash) coupled to a R446 photomultiplier (Hamamatsu Photonics). A krypton ion laser (Coherent Innova 90 K) (λ = 350 nm) was used as excitation source, keeping its maximum output power at 500 mW. All experiments measurements were performed at room temperature.

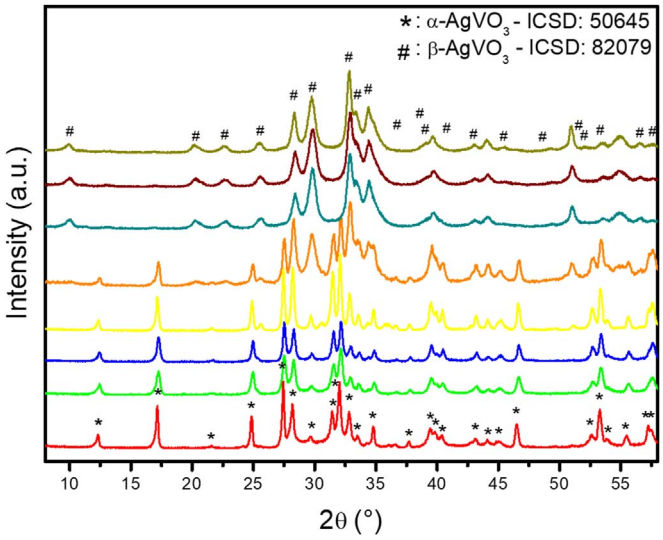

Fig. 1. XRD patterns of the $AgVO_3$ samples prepared at different synthesis temperatures.

3. Results and discussions

Fig. 1 shows the X-ray diffraction (XRD) patterns of $AgVO_3$ powders synthesized at different temperatures. Diffraction peaks for the samples obtained at 0, 15, and 25 °C can be assigned to metastable α-$AgVO_3$ with monoclinic structure (ICDS No. 50645, space group: *C2/c* (No. 15)). Peaks of other phases were not detected, indicating the high purity of the product. When the powders were obtained at 35 and 45 °C, all diffraction peaks could be indexed to the metastable α-$AgVO_3$, but the onset of the formation of β-$AgVO_3$ was observed via the weak peaks around 25.5°. The slight β-$AgVO_3$ phases might transform from the metastable α-$AgVO_3$ phase during reaction progress. However, when the synthesis temperature was increased to 55, 65, and 75 °C, all the XRD diffraction peaks could be indexed to the stable β-$AgVO_3$ phase with monoclinic structure (ICDS No. 82079, space group: Cm (No. 8)) and without the presence of a secondary phase.

The transformation from α-$AgVO_3$ to β-$AgVO_3$ with temperature can be followed by scanning electron microscopy (SEM). Fig. 2 displays a survey of the morphology and structure. As can be seen, α-$AgVO_3$ nanowires with lengths of several tens of micrometers were obtained during synthesis at 0 °C. At 15 °C, some nanowires and micro-rods with defined faces were obtained. In the sample synthesized at 25 °C, the micro-rods presented defined faces and some urchin-like microspheres were obtained by the self-assembly of micro-rods. At 35 °C, α-$AgVO_3$ crystals with urchin-like morphologies were mainly obtained, but a phase that corresponds to β-$AgVO_3$ could be observed. The phase transformation from α-$AgVO_3$ to β-$AgVO_3$ was clearly observed at 45 °C, since in addition to the micro-rods, a second morphology that corresponds to nanowires of the β-$AgVO_3$ phase was observed. According to the literature [19,22], this transformation is explained by the "ripening-splitting model" that takes place when α-$AgVO_3$ micro-rods are fragmented into β-$AgVO_3$ nanowires. During the syntheses performed at temperatures above 55 °C only nanowires were obtained, which indicates that the pure β-$AgVO_3$ phase was obtained. No significant differences were observed in the morphologies among the three samples obtained at 55, 65, and 75 °C.

The crystal structures of both β-$AgVO_3$ and α-$AgVO_3$ are known and a graphical representations are given in Fig. 3. $AgVO_3$ exhibits a rich

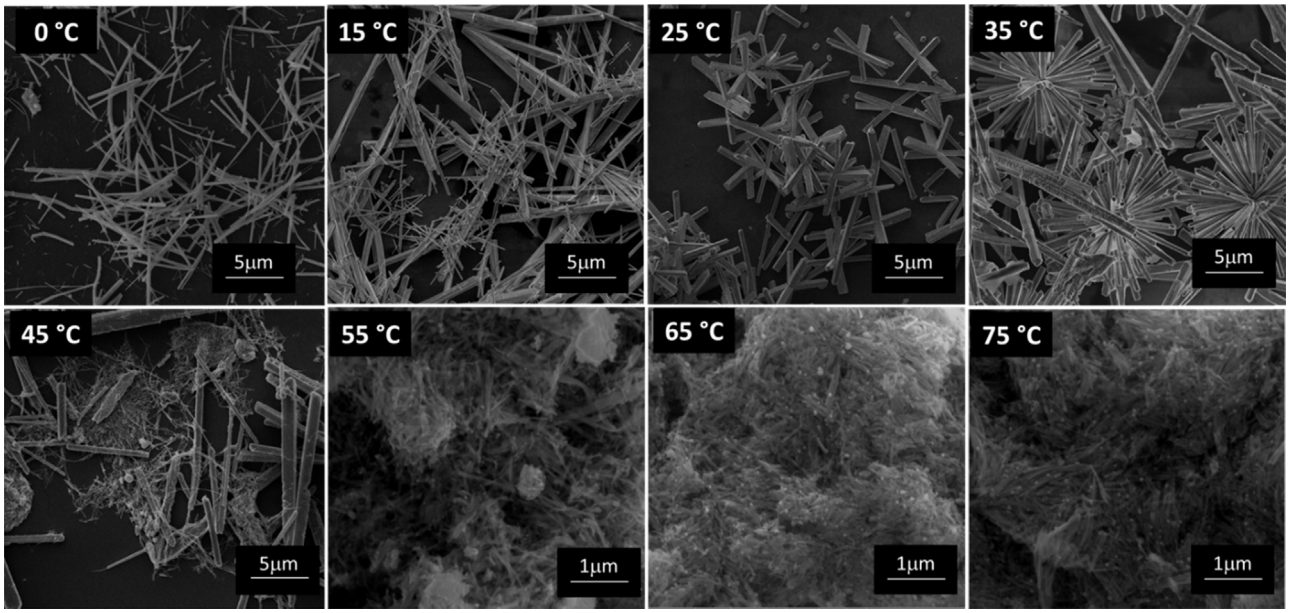

Fig. 2. Micrographs of the $AgVO_3$ samples obtained at different synthesis temperatures.

diversity of geometric and electronic structures of the [AgO_x] and [VO_4] cluster building blocks of these phases, as can be clearly seen in both α and β structures. The geometries of these clusters are reported in the Supplementary information. The number of oxygen atoms coordinating to each V cation in both β-$AgVO_3$ and α-$AgVO_3$ is four, forming [VO_4] tetrahedral clusters. Moreover, only one type of V site is present in α-$AgVO_3$, forming almost regular tetrahedra with O atoms. This is in contrast to the four types of distorted tetrahedra found in β-$AgVO_3$ (see Fig. 3). The [VO_4] clusters are distorted with four different V–O bond lengths. There are three types of Ag in β-$AgVO_3$ forming square pyramidal, octahedral, and triangular prism tetrahedral [AgO_5], [AgO_6], and [AgO_7] clusters, respectively [4]; the Ag are coordinated with six oxygen atoms to form two types of octahedral [AgO_6] clusters in α-$AgVO_3$, resulting in two types of O–Ag–O bond angles. Therefore, β-$AgVO_3$ and α-$AgVO_3$ can be composed of [VO_4] and [AgO_6], and [VO_4] and [AgO_x] (x = 5, 6, and 7) clusters, respectively.

To support the crystal structure from XRD data, first principles calculations and Raman spectroscopy were used in our previous studies. XRD can detect cation order–disorder effects as well as lattice distortion, but it is useless when investigating oxygen distortions at short range. Raman techniques are informative techniques in short-range crystal structure analysis, and are widely used in combination with first principle calculations to examine the vibration modes in the structure, phase transitions, and structural distortions. [16,21]. The distinctive properties of both phases could be ascribed to the flexibilities of the geometries in which V and Ag cations could adopt different local coordination environments. These structural features indicate that both short- and long-range ordering occur. Distortions in these clusters might induce different kinds of deformations in Ag–O and/or V–O bonds as well as O–Ag–O and/or O–V–O bond angles. Hence, the positions of O, V, and Ag atoms can vary and there is structural and electronic disorder at short range. This fact is not an accidental characteristic of a crystal,

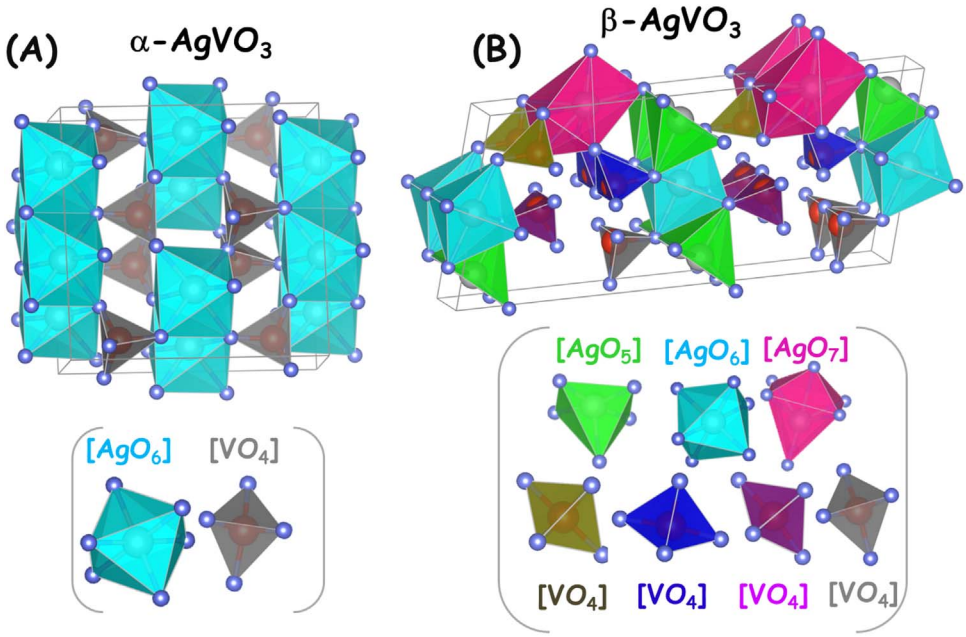

Fig. 3. Bulk structure of (A) α-$AgVO_3$ and (B) β-$AgVO_3$, in terms of its constituent clusters.

being an essential feature and is capable of drastically influencing various properties.

Structural and electronic disorder include volume, planar, line, and point defects such as voids, twins, dislocations, and vacancies, which are inevitably generated during crystal nucleation and growth [23]. These disorders have attracted continuous attention owing to their significant influence on the formation and luminescent properties of the crystal, which are crucial to applications. A change in the degree of disorder in the crystal requires a change in crystal phase and can be controlled through the temperature involved in the crystal growth conditions. In other words, the degree of disorder of a fixed crystal phase remains constant regardless of crystal growth conditions.

An understanding of the transformation from α to β phase of $AgVO_3$ induced by temperature is directly related to the question of whether the basic nature of structural and electronic properties depends on short-range order (localized electronic states) and/or long-range order (extended electronic states and well-defined energy bands).

In the co-precipitation method, the crystallization process is controlled by the solvent, precursor, and temperature. These affect kinetic or/and thermodynamic factors, and in the present case the reaction temperature is the key factor determining the formation of β-$AgVO_3$ or α-$AgVO_3$ crystals. Temperature has a strong impact on local coordination, bond lengths, and bond angles of V and Ag cations in the clusters. The main structural difference between these $AgVO_3$ phases is given by displacements of the networks of former clusters, $[VO_4]$, and modifier clusters $[AgO_x]$ (x = 5, 6, and 7). Therefore, consideration of the local atomic structure is essential to fully understand the phase transition.

NH_4VO_3(aq) and $AgNO_3$(aq) are the starting materials for the synthesis of α and β single-crystalline $AgVO_3$ phases by the co-precipitation method. NH_4^+(aq) is released from the dissociation of NH_4VO_3(aq), and it can react with the Ag^+ cation to form the $[Ag(NH_3)_2(H_2O)_4]^+$ complex. $[Ag(NH_3)_2(H_2O)_4]^+$ and VO_3^-(aq) are the precursors of the $[AgO_x]$ (x = 5, 6, 7) and $[VO_4]$ clusters in the solid state, respectively.

The mechanism for the formation of crystals in liquid solution is complex but commonly driven by the intrinsic properties of the crystal and the environment. Fig. 4 illustrates the formation mechanism of α- or β-$AgVO_3$ crystals. Generally, a crystalline phase is generated as a result of ion aggregation processes in solution that lead to the formation of nuclei, associating to pre-nucleation clusters [24]. $[Ag(NH_3)_2(H_2O)_4]^+$ (aq) and VO_3^-(aq) rearrange to form amorphous crystal nuclei. In aqueous environments, water molecules donate oxygen atoms for oxide formation via hydrolysis and condensation processes. From here, $[VO_4]$ and $[AgO_x]$ (x = 5, 6, and 7) are formed and they gain a certain size after a sufficient time to enable growth into macroscopic crystals. From these clusters, we can obtain mechanistic insights to explain the synthesis and experimental observations. To propose a formation mechanism, concerted and cooperative processes have to be separated in time and split into a sequence of individual reaction steps, and chemical reactions related to cluster aggregation, α- and β- phase formation, and transformation. First, the reaction between the $[AgO_x]$ and $[VO_4]$ complex clusters occurs locally to form the initial crystal nucleus. Nucleation finishes immediately in oversaturated solutions and the crystal growth process begins. V cations only form $[VO_4]$ complex clusters, and Ag cations assume an octahedral coordination to form $[AgO_6]$ complex clusters when the metastable α-$AgVO_3$ is obtained; to form β-$AgVO_3$, beside the $[AgO_6]$ complex clusters, two other coordination clusters are observed: $[AgO_5]$ and $[AgO_7]$.

On the basis of experimental results, it was found that tuning the temperature was a crucial step in the polymorphic control of $AgVO_3$ preparation. Increasing the temperature favors structural and electronic disorder, and induces the presence of under- and over-coordinated Ag ions ($[AgO_5]$ and $[AgO_7]$), hence the formation of β-phase is favored. In contrast, the more ordered α-phase is obtained at lower temperatures.

In the $[Ag(NH_3)_2(H_2O)_4]^+$(aq) complex, Ag-N bonds are stronger than Ag-O bonds. At low temperature, the release of Ag cations is more difficult and formation of the α-$AgVO_3$ structure via linear organization is favored. At high temperature, the vibration increases and makes it easier to liberate Ag from $[Ag(NH_3)_2(H_2O)_4]^+$(aq) and to enhance the formation of the β-$AgVO_3$ phase with more disorder over both short and medium distances.

Such variations in the atomic and electronic structure are expected to be responsible for kinetic and thermodynamic control of the synthesis of α- and β-$AgVO_3$ polymorphs. Higher temperatures generally favor thermodynamic kinetic control (β-$AgVO_3$), whereas lower temperatures favor kinetic reaction control (α-$AgVO_3$). Fine-tuning of the synthesis temperature controls the transformation from the metastable phase to the stable phase.

The formation of α- or β-$AgVO_3$ is dependent on the relative phase stability (thermodynamic factor) and the rate of product formation (kinetic factor). Order/disorder of the constituent clusters affects the selective synthesis of α- or β-$AgVO_3$. α-$AgVO_3$ has a more ordered structure than β-$AgVO_3$. The β phase is the most stable form of $AgVO_3$, but a high reaction temperature is necessary to overcome the larger activation barrier, as pointed out in Fig. 5, and Fig. S1 in the Supporting Information. The formation of α-$AgVO_3$ takes place along a lower activation barrier than β-$AgVO_3$, as illustrated in Fig. 5.

At low temperature, rearrangements between $[VO_4]$ and $[AgO_6]$ clusters take place along the reaction pathway via transition state TS1 to render the metastable α-$AgVO_3$. In contrast, at higher temperatures, $[AgO_6]$ complex clusters tend to disorganize themselves, and new clusters are formed with different coordination values: $[AgO_5]$ and $[AgO_7]$; these three clusters rearrange with $[VO_4]$ to obtain the more disordered stable polymorph, β-$AgVO_3$ via transition state TS2. In addition, both α-$AgVO_3$ and β-$AgVO_3$ can be connected via transition state TS3 without the need for return to the initial state of nucleation; this path explains the temperature-induced phase transformation. We attribute the greater stability of β-$AgVO_3$ with respect to α-$AgVO_3$ to the high degree of structural and electronic disorder. Specifically,

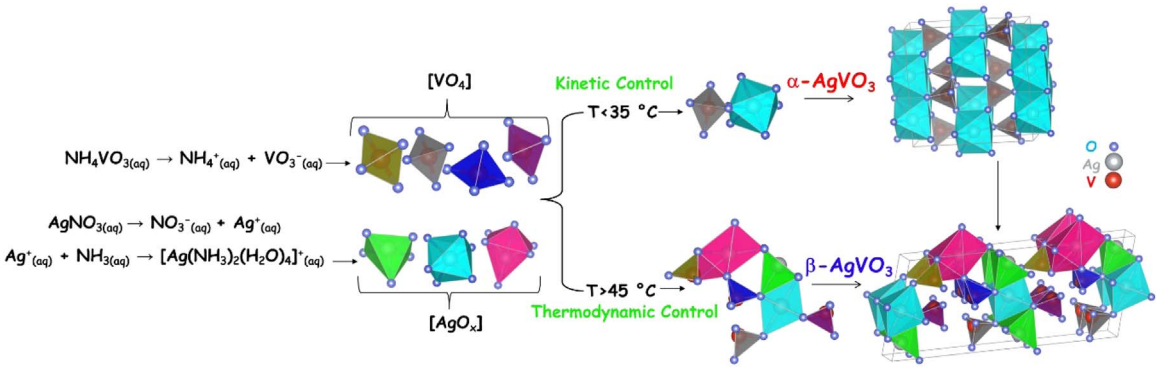

Fig. 4. Schematic representation for the formation mechanism proposed for the α-$AgVO_3$ and β-$AgVO_3$ crystals.

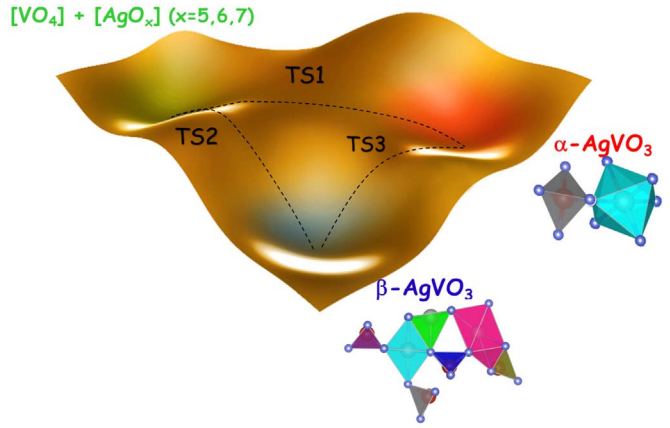

Fig. 5. Reaction coordinate diagram for the formation of α-$AgVO_3$ and β-$AgVO_3$ crystals.

temperature acts on the internal energy of the system changing the kinetic energy. Finally, we recognize that other factors influence the selective synthesis of α- and β-$AgVO_3$ crystals such as solvent, pH, supersaturation, and solubility, but the above mechanism is in good agreement with our experiment.

The conduction band of $AgVO_3$ is controlled by the hybridization of V 3d orbitals with Ag 5s orbitals, while the valence band is associated with O 2p orbitals hybridized with Ag 3d orbitals, yielding a narrow band gap and highly dispersed conduction and valence bands. [16,21,25,26]. According to the broadband model, the PL emissions of a semiconductor are associated with distortions in the crystalline lattice. After the semiconductor is excited, the recombination process occurs due to these distortions. The electronic properties can thus be changed by structural distortions. In our case, PL emissions are very sensitive to changes in the first coordination sphere of Ag and V cations, i.e., Ag and V cations show distinct changes in the emission/excitation spectra and excited state dynamics with changes in their local symmetries.

We reported the temperature and phase dependences of PL emissions from as-synthetized $AgVO_3$ samples. Fig. 6a shows the $AgVO_3$ phase dependence of the PL emission, which was observed at the maximum displacement as the $AgVO_3$ synthesis temperature increases, and thus with the change of phase from α- to β-$AgVO_3$. Hence, expansion of the band gap induced the increase of energy between the defect deep levels and the valence band, which caused the blue shift of the emission (Fig. 6a).

Each peak of the PL spectrum was deconvolved (see Fig. 6b). Initially, the emission maximum of α-$AgVO_3$ occurs predominantly at 705 nm, which is related to oxygen vacancies [AgO_6]. With increase in temperature, the band at 458 nm which is associated with β-$AgVO_3$ formation becomes more evident. The blue emission is a consequence of the presence of distorted [AgO_x] (x = 5, 6, and 7) clusters and four types of distorted [VO_4] clusters in the β-$AgVO_3$ structure.

The color of the sample was evaluated using the Commission Internationale de l´Éclairage (CIE) chromaticity diagram; the results are presented in Fig. 7. The α-$AgVO_3$ samples obtained at 0, 15, 25, and 35 °C, exhibited red colors while the sample obtained at 45 °C (composed of a mixture of α-$AgVO_3$ and β-$AgVO_3$) displayed a purplish pink color. With further increase in the synthesis temperature, β-$AgVO_3$ was obtained and shift from green to blue was observed. These outcomes indicate that $AgVO_3$ is appropriate for applications in visible lamps, displays, and other optical devices. Moreover, the color of the light can be varied with the temperature of synthesis and therefore with the obtained phase (α, β, or the mixture of α and β).

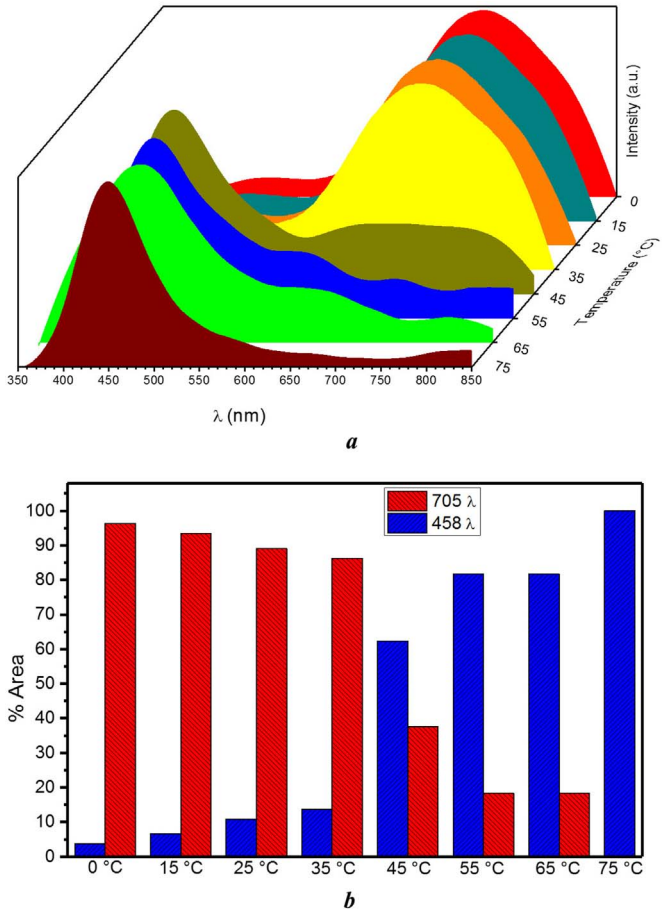

Fig. 6. ***a***: PL emission dependence of the $AgVO_3$ samples obtained at different synthesis temperatures. ***b:*** Percentage of area obtained with deconvolution of the PL spectra emission.

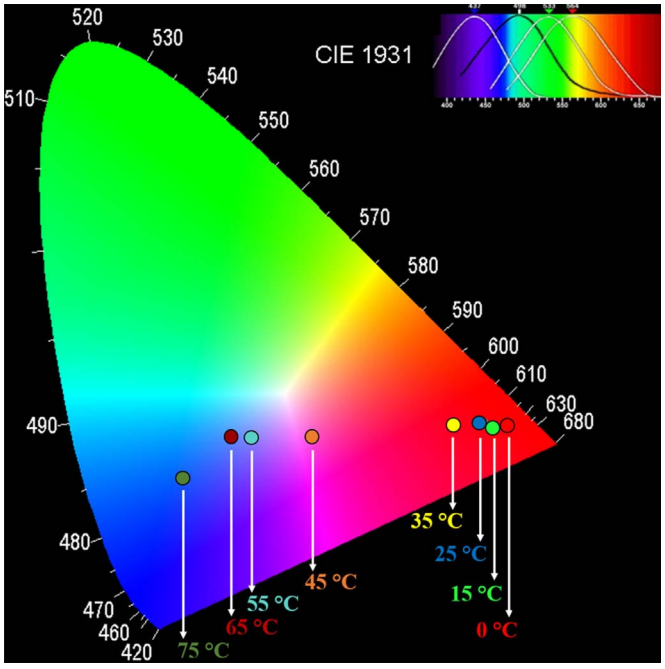

Fig. 7. CIE chromaticity diagram of $AgVO_3$ samples obtained at different synthesis temperatures.

4. Conclusions

Temperature is a versatile thermodynamic parameter that can be exploited in the pursuit of new materials. Polymorphism opens up the possibility of fine-tuning crystal packing without changing the chemical structure and offers a new avenue for optimizing device performance. Metastable polymorphs of complex oxides are interesting because of their ability to produce unique geometries and electronic structures with different bonding environments than the stable phase under normal conditions. To this end, the synthesis of metastable phases of a given material has recently experienced heightened interest. For many technological applications, it is mandatory to find more details from the different phases and their temperature-induced transformations. Specific temperature increase rates may trigger unexpected solid-state transformations producing otherwise inaccessible phases.

Phase transformations in solid-state materials are often rich, consisting of a hierarchy of rearrangements ranging from those occurring at the atomic level to those taking place at nano- and macroscopic length scales. Mechanistic understanding of these complex phase transformations and the control of their outcomes are central to materials science. The ability to measure and tune chemical thermodynamics and kinetics in the solid-state is at the heart of these aims. Here, we report a co-precipitation method for the polymorphic control of the α- and β-$AgVO_3$ polymorphs of $AgVO_3$ crystals with monoclinic structures by tuning the temperature. Phase transformation caused by the increase in synthesis temperature and can be ascribed to the higher thermodynamic stability of β-$AgVO_3$ than that of α-$AgVO_3$. Analysis of the PL emission as a function of temperature renders a wide range of color from red to blue. Temperature-induced transitions where the $AgVO_3$ system undergoes structural and electronic changes are evidenced from the PL measurements. Our understanding of this behavior relies on our ability to describe the structural and electronic characteristics such as the short-range order/disorder of the [VO_4] and [AgO_x] (x = 5, 6, and 7) cluster building blocks of the monoclinic structures of both phases. These clusters are the species that truly react in this process and the mechanistic aspects of this phase transformation are understood in detail and dictate the product formation and kinetics of reactions. This mechanistic understanding has allowed the development of strategies to control the phase in the final product structure. The findings reported in this work highlight the capabilities and potential challenges of $AgVO_3$ polymorphs, and provide highly valuable optical properties, opening a wide space in generating photoluminescent materials.

Acknowledgements

The authors acknowledge the financial support of agencies: CAPES (PNPD – 1268069), FAPESP (2013/07296-2; 2013/26671-9), CNPq (304531/2013-8). J.A. acknowledges Generalitat Valenciana for Prometeo II/2014/022, ACOMP/2014/270, and ACOMP/2015/1202, and Ministerio de Economia y Competitividad (Spain) project CTQ2015-65207-P, Programa de Cooperación Científíca con Iberoamerica (Brasil) of Ministerio de Educación (Spanish Brazilian program PHBP14-00020).

Appendix A. Supporting information

Supplementary data associated with this article can be found in the online version at http://dx.doi.org/10.1016/j.ceramint.2017.12.161.

References

[1] A.J. Cruz-Cabeza, S.M. Reutzel-Edens, J. Bernstein, Facts and fictions about polymorphism, Chem. Soc. Rev. 44 (23) (2015) 8619–8635.
[2] E. Mitscherlich, Sur la Relation qui existe entre la forme cristalline et les propriétés chimiques, Ann. De. Chim. Et. De. Phys. 19 (1822) 69.
[3] U. Schubert, N. Hüsing, Synthesis of Inorganic Materials, 3 ed. Weinheim, 2012.
[4] K.J. Takeuchi, A.C. Marschilok, S.M. Davis, R.A. Leising, E.S. Takeuchi, Silver vanadium oxides and related battery applications, Coord. Chem. Rev. 219 (2001) 17.
[5] H. Zeng, Q. Wang, Y. Rao, Ultrafine β-AgVO3nanoribbons derived from α-AgVO3nanorods by water evaporation method and its application for lithium ion batteries, RSC Adv. 5 (4) (2015) 3011–3015.
[6] J. Xu, C. Hu, Y. Xi, B. Wan, C. Zhang, Y. Zhang, Synthesis and visible light photocatalytic activity of β-AgVO3 nanowires, Solid State Sci. 14 (4) (2012) 535–539.
[7] S. Liang, J. Zhou, A. Pan, Y. Li, T. Chen, Z. Tian, H. Ding, Facile synthesis of β-AgVO3 nanorods as cathode for primary lithium batteries, Mater. Lett. 74 (2012) 176–179.
[8] R.D. Holtz, B.A. Lima, A.G. Souza Filho, M. Brocchi, O.L. Alves, Nanostructured silver vanadate as a promising antibacterial additive to water-based paints, Nanomedicine: Nanotechnol. Biol. Med. 8 (6) (2012) 935–940.
[9] C. Han, Y. Pi, Q. An, L. Mai, J. Xie, X. Xu, L. Xu, Y. Zhao, C. Niu, A.M. Khan, X. He, "Substrate-assisted self-organization of radial beta-AgVO(3) nanowire clusters for high rate rechargeable lithium batteries, Nano Lett. 12 (9) (2012) 4668–4673.
[10] F. Cheng, J. Chen, Transition metal vanadium oxides and vanadate materials for lithium batteries, J. Mater. Chem. 21 (27) (2011) 9841.
[11] L. Mai, L. Xu, Q. Gao, C. Han, B. Hu, Y. Pi, Single beta-AgVO3 nanowire H2S sensor, Nano Lett. 10 (7) (2010) 2604–2608.
[12] S.J. Bao, Q.L. Bao, C.M. Li, T.P. Chen, C.Q. Sun, Z.L. Dong, Y. Gan, J. Zhang, Synthesis and electrical transport of novel channel-structured beta-AgVO3, Small 3 (7) (2007) 1174–1177.
[13] S. Kittaka, K. Matsuno, H. Akashi, Crystal structure of a-AgVO3 and phase relation of AgVO3, J. Solid State Chem. 142 (1999) 7.
[14] M.R. Parida, C. Vijayan, C.S. Rout, C.S. Suchand Sandeep, R. Philip, Enhanced optical nonlinearity in β-AgVO3 nanobelts on decoration with Ag nanoparticles, Appl. Phys. Lett. 100 (12) (2012) 121119.
[15] S. Sharma, M. Panthöfer, M. Jansen, A. Ramanan, Ion exchange synthesis of silver vanadates from organically templated layered vanadates, Mater. Chem. Phys. 91 (2–3) (2005) 257–260.
[16] R.C. Oliveira, M. Assis, M.M. Teixeira, M.D.P. da Silva, M.S. Li, J. Andres, L. Gracia, E. Longo, An experimental and computational study of β-$AgVO_3$: optical properties and formation of Ag nanoparticles, J. Phys. Chem. C. 120 (22) (2016) 12254–12264.
[17] G.-T. Pan, M.-H. Lai, R.-C. Juang, T.-W. Chung, T.C.K. Yang, Preparation of visible-light-driven silver vanadates by a microwave-assisted hydrothermal method for the photodegradation of volatile organic vapors, Ind. Eng. Chem. Res. 50 (5) (2011) 2807–2814.
[18] D.P. Singh, K. Polychronopoulou, C. Rebholz, S.M. Aouadi, Room temperature synthesis and high temperature frictional study of silver vanadate nanorods, Nanotechnology 21 (32) (2010) 325601.
[19] T. Chen, M. Shao, H. Xu, C. Wen, S.T. Lee, Control over the crystal phase, crystallinity, morphology of AgVO3 via protein inducing process, J. Colloid Interface Sci. 366 (1) (2012) 80–87.
[20] D. McNulty, Q. Ramasse, C. O'Dwyer, The structural conversion from α-$AgVO_3$ to β-$AgVO_3$ Ag nanoparticle decorated nanowires with application as cathode materials for Li ion batteries, Nanoscale 89 (2016).
[21] R.C. Oliveira, C.C. Foggi, M.M. Teixeira, M.D. da Silva, M. Assis, E.M. Francisco, B.N. Pimentel, P.F. Pereira, C.E. Vergani, A.L. Machado, J. Andres, L. Gracia, E. Longo, Mechanism of Antibacterial Activity via Morphology Change of alpha-AgVO3: theoretical and Experimental Insights, ACS Appl. Mater. Interfaces 9 (13) (2017) 11472–11481.
[22] S. Zhang, W. Li, C. Li, J. Chen, Synthesis, characterization, and electrochemical properties of $Ag_2V_4O_{11}$ and $AgVO_3$ 1-D nano/microstructures, J. Phys. Chem. B 110 (2006) 8.
[23] H. Klapper, Generation and propagation of defects during crystal growth, in: G. Dhanaraj, K. Byrappa, V. Prasad, M. Dudley (Eds.), Springer Handbook of Crystal Growth, 1 Springer-Verlag Berlin Heidelberg, Berlin, 2010, p. 1818.
[24] D. Gebauer, M. Kellermeier, J.D. Gale, L. Bergstrom, H. Colfen, Pre-nucleation clusters as solute precursors in crystallisation, Chem. Soc. Rev. 43 (7) (2014) 2348–2371.
[25] H.G. Na, S.-W. Choi, S. Park, S.J. Hwang, M.S. Cho, Y. Noh, H.J. Kim, D. Lee, C. Jin, One-to-one correspondence growth mechanism of gourd-like SiOx nanotubes, Cryst. Growth Des. 16 (6) (2016) 3081–3086.
[26] K.A. Hengge, C. Heinzl, M. Perchthaler, S. Geiger, K.J.J. Mayrhofer, C. Scheu, Growth of porous platinum catalyst structures on tungsten oxide support materials: a new design for electrodes, Cryst. Growth Des. 17 (4) (2017) 1661–1668.